THE JOURNAL OF BIOLOGICAL CHEMISTRY
Vol. 279, No. 27, Issue of July 2, pp. 28165–28173, 2004

Printed in U.S.A.

Subunit Composition of NDH-1 Complexes of *Synechocystis* sp. PCC 6803

IDENTIFICATION OF TWO NEW *ndh* GENE PRODUCTS WITH NUCLEAR-ENCODED HOMOLOGUES IN THE CHLOROPLAST Ndh COMPLEX*

Received for publication, February 2, 2004, and in revised form, March 24, 2004
Published, JBC Papers in Press, April 21, 2004, DOI 10.1074/jbc.M401107200

Peerada Prommeenate‡§, Adrian M. Lennon‡, Christine Markert¶‖, Michael Hippler¶‖, and Peter J. Nixon‡**

From the ‡Department of Biological Sciences, Wolfson Laboratories, Imperial College London, South Kensington campus, London SW7 2AZ, United Kingdom and the ¶Lehrstuhl für Pflanzenphysiologie, Friedrich-Schiller-Universität Jena, 07743 Jena, Germany

Cyanobacteria contain several genes, annotated *ndh*, whose products show sequence similarities to subunits found in complex I (NADH:ubiquinone oxidoreductase) of eubacteria and mitochondria. However, it is still unclear whether the cyanobacterial *ndh* gene products actually form a single large protein complex or exist as smaller independent complexes. To address this, we have constructed a strain of *Synechocystis* sp. PCC 6803 in which the C terminus of the NdhJ subunit was fused to an His_6 tag to aid isolation. Three major NdhJ-containing complexes were resolved by blue native polyacrylamide gel electrophoresis, with approximate apparent molecular masses of 460, 330, and 110 kDa. N-terminal sequencing and mass spectrometry revealed that the 460-kDa complex contained ten annotated *ndh* gene products. Detergent-induced fragmentation experiments indicated that the 460-kDa complex was composed of hydrophobic (150 kDa) and hydrophilic (110–130 kDa) modules similar to that found in the minimal form of complex I found in *Escherichia coli*, except that the electron input module was not conserved. The difference in size between the 460- and 330-kDa complexes is attributed to differences in the stoichiometry of the hydrophilic and hydrophobic modules in the complex, either 2:1 or 1:1, respectively. We have also detected the presence of two new Ndh subunits (slr1623 and sll1262) that are unrelated to subunits in the eubacterial complex I but which have homologues in the closely related chloroplast Ndh complex of maize (Funk, E., Schäfer, E., and Steinmüller, K. (1999) *J. Plant Physiol.* 154, 16–23). The presence of these additional subunits might reflect the use by the NDH-1 and Ndh complexes of a different, so far unidentified, electron input module.

An interesting feature of cyanobacteria is that the thylakoid membrane contains both photosynthetic and respiratory complexes (1). Analysis of the genome sequence of *Synechocystis* sp. PCC 6803 and other cyanobacteria has led to the hypothesis that it contains a type I NAD(P)H dehydrogenase, designated NDH-1, similar in function to complex I (NADH:ubiquinone oxidoreductase) found in mitochondria and eubacteria (2).

Based on sequence comparisons, genes encoding 11 potential Ndh subunits have been identified in the *Synechocystis* 6803 genome (*ndhA–K*) (2). Evolutionary considerations suggest that complex I consists of three distinct structural elements or modules: an NADH-oxidizing sub-complex, an interconnecting hydrophilic fragment containing a number of Fe-S redox centers, and a hydrophobic membrane domain possibly involved in the pumping of protons (3–5). By analogy, the cyanobacterial *ndh* gene products could form the interconnecting hydrophilic fragment (NdhH, -I, -J, and -K) and the membrane domain (NdhA–F) (6) of a putative NDH-1 complex. However, *Synechocystis*, like the related Ndh complex in chloroplasts (7), does not have obvious homologues to the NuoE, -F, and -G subunits of *Escherichia coli*, which are responsible for binding and oxidizing NADH. It is possible that subunits of the bidirectional hydrogenase might act as substitutes (8, 9), or that there might be a different type of electron input module, which may or may not oxidize NAD(P)H. Alternatively, the putative NDH-1 complex might act as a ferredoxin:plastoquinone oxidoreductase and lack a specific electron input module (6). As yet the substrate specificity of the putative NDH-1 complex is unclear with NADH (10, 11), NADPH (11, 12), and reduced ferredoxin (11) all implicated.

Most attention has so far focused on the construction and physiological characterization of various *ndh* mutants. For instance, the *ndhB* insertion mutant, M55, is impaired in dark respiration and shows slower rates of re-reduction of $P700^+$, the oxidized primary electron donor of photosystem one, in the dark in intact cells (13, 14). This has led to the assumption that a putative NDH-1 complex functions in respiration and cyclic electron flow around photosystem one by acting as a plastoquinone reductase. However, the impaired rates of plastoquinone reduction seen in the *ndh* mutants might actually be due to low levels of succinate in these strains, which limit the respiratory activity of the thylakoid succinate:plastoquinone oxidoreductase (15).

The lack of a consistent phenotype for various *ndh* mutants has led to suggestions that there might be various types of NDH-1 complex *in vivo* each with different activities (16). For instance, although an *ndhC* insertion mutant can grow in air, *ndhB* and *ndhK* mutants require high levels of CO_2 for growth (13, 17), and the *ndhH* gene appears to be absolutely required for cell viability even at high concentrations of CO_2 (18).

* This work was supported in part by grants from the Biotechnology and Biological Sciences Research Council (to P. J. N.) and the Federal State of Thüringen, Germany (to M. H.). The costs of publication of this article were defrayed in part by the payment of page charges. This article must therefore be hereby marked "*advertisement*" in accordance with 18 U.S.C. Section 1734 solely to indicate this fact.

§ Recipient of a Royal Thai scholarship.
‖ Current address: Dept. of Biology, University of Pennsylvania, Philadelphia, PA 19104.
** To whom correspondence should be addressed. Tel.: 44-20-7594-5269; Fax: 44-20-7594-5267; E-mail: p.nixon@imperial.ac.uk.

Some of the *ndh* genes are also found as multigene families. According to CyanoBase, there are six copies of the *ndhD* gene and three copies of the closely related *ndhF* gene (19). Mutagenesis studies indicate that NdhD1 and NdhD2 are important for cyclic electron flow, whereas NdhD3/NdhF3 and NdhD4/NdhF4 are important for the inducible and constitutive transport, respectively, of inorganic carbon into the cell (20–23). Whether the NdhD3/NdhF3 and NdhD4/NdhF4 subunits are part of larger NDH-1 complexes or exist as independent complexes is again unclear, although recent evidence supports the latter possibility (24).

Attempts to isolate and characterize the subunit composition of the putative NDH-1 complex have so far met with little success. Only hydrophilic sub-complexes of various degrees of purity have been isolated (12, 25). Steinmüller and colleagues (25) used antibodies raised against NdhK to immunoprecipitate an additional seven subunits from detergent-solubilized membrane extracts. N-terminal sequencing identified the presence of NdhH, NdhK, NdhI, and NdhJ. At the time the identity of the remaining subunits was unclear but comparison of their partial N-terminal sequences to the more recently acquired genome sequence now suggests that 21- and 18-kDa subunits are actually ribosomal proteins (L5 and L9, respectively) and that a 14-kDa subunit is encoded by the open reading frame slr1623. Given that the ribosomal proteins are presumably contaminants, it remains uncertain whether slr1623 is part of the NDH-1 complex.

More recently a 380-kDa complex showing NADPH:ferricyanide oxidoreductase activity was isolated from *Synechocystis* 6803 (12). SDS-PAGE indicated the presence of at least nine protein bands with sizes ranging from 120 to 10 kDa. NdhH was found by immunoblotting to be present in the preparation, but the hydrophobic NdhA and NdhB subunits were absent. Although the NADPH:ferricyanide oxidoreductase activity was assumed to be due to the NDH-1 sub-complex, definitive evidence for this assignment was lacking.

A major question that needs to be addressed, therefore, is whether the *ndh* gene products actually assemble into a large protein complex. Given current ideas on the modular evolution of complex I, it is conceivable that the *ndh* gene products could form distinct modules or sub-complexes that do not interact (4, 5). This is highlighted by recent studies that have suggested that the NdhB and NdhH subunits are differentially expressed (26) and are not members of the same complex (18). Thus the major aims of this work were to investigate whether the *ndh* gene products assemble into structural modules within a larger complex, and if so, whether there were additional hitherto unidentified Ndh subunits that might give clues to the nature of the electron input module.

To help achieve these goals, we have generated a strain of *Synechocystis* 6803 in which the NdhJ subunit contains a His tag at its C terminus. The choice of the NdhJ subunit was guided by tagging experiments involving its closest relative in the yeast *Yarrowia lipolytica* (27). A combination of anion-exchange chromatography and immobilized Ni-affinity chromatography plus blue native (BN-PAGE)[1] has allowed us to characterize different NdhJ-containing complexes from *Synechocystis* 6803.

Our results provide the first evidence that the Ndh subunits are indeed organized into hydrophobic and hydrophilic subcomplexes, as observed for other types of complex I, and do associate to form large complexes. Importantly we have identified two new Ndh subunits in *Synechocystis* 6803 that are not found in *E. coli* complex I. By comparison to earlier N-terminal sequence data, we conclude that closely related proteins found in higher plants are the first examples of nuclear-encoded components of the chloroplast Ndh complex. The module or subunit that feeds electrons into both types of complex still remains unclear. We discuss the possibility that it might be related to the electron input device found in archaebacterial coenzyme $F_{420}H_2$ dehydrogenases.

EXPERIMENTAL PROCEDURES

Construction of His-tagged NdhJ Strain—Overlap-extension PCR was used to insert a His_6 tag at the C terminus of NdhJ (28). Primers used were $ndhJ_{for}$ (5′-GGG GGA TCC AGG ATA CCC GTA ACC CGG AAG-3′), $ndhJ_{rev}$ (5′-GGG CTC GAG CAG CCA TCC TTC AAA ACC CGT-3′), His_{for} (5′-CAT CAC CAT CAC CAT CAC TAG TCC CGG TCG CAC ACG GCA AAA-3′), and His_{rev} (5′-CTA GTG ATG GTG ATG GTG ATG ATA GGC ATC CTG GAG TTC-3′). Briefly, two DNA fragments were generated using *Synechocystis* 6803 genomic DNA as a template and the primer combinations $ndhJ_{for}$/His_{rev} and His_{for}/$ndhJ_{rev}$. The purified fragments were then used as templates in a new PCR reaction using primers $ndhJ_{for}$ and $ndhJ_{rev}$ to amplify the final fused product, which was cloned into pGEM-T Easy (Promega, UK) to generate plasmid pNdhJ-His. Overall a 1.24-kb fragment was amplified extending from bases 1,876,591 to 1,877,809 of the genome sequence (2). A chloramphenicol-resistance cassette was inserted into a HincII site, 102 bp downstream of the stop codon of *ndhJ*, to generate plasmid pNdhJ-Hiscam. Plasmids were sequenced to confirm no unwanted base changes. The glucose-tolerant strain of *Synechocystis* 6803 was transformed with pNdhJ-Hiscam according to Ref. 29, and chloramphenicol-resistant colonies were analyzed by PCR to confirm incorporation of His-tagged *ndhJ* into the chromosome. One such strain, NdhJ-His, was used for isolation of the NDH-1 complex.

Purification of the His-tagged NdhJ Preparation from Synechocystis sp. PCC 6803—Strain NdhJ-His was grown in BG-11 medium supplemented with 5 mM glucose at constant light (20 μmol.m^{-2}.s^{-1}) and with air bubbling (29). Cultures (16 liters) were harvested in their exponential growth phase by centrifugation at 8,000 × *g* (JA21 rotor, BD Biosciences) for 10 min at 4 °C. The pellet was washed twice in 500 ml of washing buffer (20 mM sodium phosphate, pH 7.5, 5% (v/v) glycerol, 5 mM $MgCl_2$, and 10 mM NaCl). The cells were broken by resuspending the pellet in 50 ml of washing buffer (containing 1 mM benzamidine, 1 mM aminocaproic acid, 1 mM Pefabloc, and 50 μg/ml DNase) and by two consecutive passages through a French Press at 2,000 p.s.i. Cell debris and unbroken cells were removed by centrifugation for 5 min at 3,000 × *g* (JA14 rotor, BD Biosciences). The thylakoids were collected from the supernatant by centrifuging at 100,000 × *g* for 20 min (Ti-70 rotor, BD Biosciences), and the resulting thylakoid pellet was resuspended in UnoQ buffer (5 mM $MgSO_4$, 20 mM MES, pH 6.5, 10 mM $MgCl_2$, 10 mM $CaCl_2$, 25% (v/v) glycerol, and 0.03% (w/v) *n*-dodecyl-β-D-maltoside (β-DM)) to a concentration of 0.5 mg/ml chlorophyll. Membranes were stored at −80 °C. Thylakoids were solubilized using β-DM (Calbiochem). A 10% (w/v) stock solution of β-DM in UnoQ buffer was added dropwise to the thylakoid membrane suspension (typically 20 mg of chlorophyll) at a chlorophyll concentration of 0.5 mg/ml to give a final concentration of 1% (w/v) β-DM and 0.45 mg/ml chlorophyll. This process was performed for 10 min in the dark at 4 °C with gentle stirring. The suspension was then centrifuged at 100,000 × *g* (Ti-70 rotor, BD Biosciences) for 30 min at 4 °C to remove unsolubilized membranes. The solubilized thylakoid extract was applied at a flow rate of 2 ml/min to a 25-ml Q-Sepharose™ High Performance (Amersham Biosciences) vertical column, previously equilibrated with UnoQ buffer. The column was washed with 2 column volumes of UnoQ buffer, and the column was eluted with an $MgSO_4$ gradient (5–200 mM) in the same buffer over 16 column volumes. The unbound fraction and the fractions containing the eluted protein were collected and kept at −80 °C for further analysis. Immunoblots revealed that NdhI and NdhJ were co-eluted, peaking at a salt concentration of ~100 mM $MgSO_4$. His-tagged NdhJ was purified by affinity chromatography using Ni^{2+}-NTA-agarose resin (Qiagen). Ni^{2+}-NTA-agarose was incubated with Binding Buffer (20 mM MES, pH 6.5, 60 mM $MgSO_4$, 10 mM $MgCl_2$, 10 mM $CaCl_2$, 25% (v/v) glycerol, and 0.03% (w/v) β-DM). Pooled fractions from the Q-Sepharose column (~40 ml) were added to the column material, and binding was achieved by mixing in a 50-ml tube (using a rotator mixer) at 4 °C for 2 h. Approximately 0.3 ml of resin was used per milliliter of pooled fraction. The

[1] The abbreviations used are: BN-PAGE, blue native PAGE; MES, 4-morpholineethanesulfonic acid; β-DM, *n*-dodecyl-β-D-maltoside; Ni-NTA, nickel-nitrilotriacetic acid; Tricine, *N*-[2-hydroxy-1,1-bis(hydroxymethyl)ethyl]glycine; MS, mass spectrometry; CBB, Coomassie Brilliant Blue; WT, wild type.

column material was resettled and washed with Binding Buffer containing imidazole (5 and 10 mM) to remove weakly bound proteins. The His-tagged NdhJ protein was eluted using Binding Buffer containing 100 mM imidazole. The purified proteins were then diluted 50-fold with Binding Buffer to reduce the imidazole concentration and concentrated using Amicon® Ultra-15 units (100-kDa molecular mass cut-off) and stored at −80 °C. Protein concentrations were determined using a Bio-Rad protein assay kit, and chlorophyll was determined according to a previous study (30). Approximately 1.5 mg of the final His-tagged NdhJ preparation was obtained from 250 mg of thylakoid protein.

SDS-PAGE and Immunoblotting—Proteins were electrophoresed through 12% (w/v) polyacrylamide gels fused to a 5% (w/v) polyacrylamide stacking gel, using a Tris-Tricine buffer system (31). Pre-stained and unstained protein markers were purchased from Bio-Rad Ltd. UK and Invitrogen, respectively. Immunoblotting was performed as described previously (32) using the SuperSignal® West Pico Chemiluminescent Substrate detection system (Pierce Biotechnology, Perbio Science Ltd., UK). Antibodies specific for NdhI and NdhJ are described in a previous study (32). Anti-peptide antibodies specific for NdhF3 are described in a previous study (24) and were kindly made available by Professor Eva-Mari Aro (University of Turku, Finland). Silver staining was performed according to a previous study (33).

N-terminal Protein Sequencing—The samples for protein sequencing were electroblotted to polyvinylidene difluoride membrane (Bio-Rad Ltd., UK) according to a previous study (34). The membrane was washed three times with water and stained with 0.2% (w/v) Coomassie Blue R250 in 40% (v/v) methanol/H_2O. The membrane was destained in 50% (v/v) methanol/H_2O and dried. The protein spots of interest were cut out and sequenced by Dr. Jeff Keen at the School of Biochemistry and Molecular Biology, University of Leeds using the Edman degradation method.

Liquid Chromatography-Mass Spectrometry and Data Analysis—Samples for tandem mass spectrometry were prepared by tryptic in-gel digestion of excised protein bands/spots according to a previous study (35). The samples were dried and stored at −80 °C until further use. For MS/MS analysis the dried samples were diluted in 10 μl of buffer A (0.1% (v/v) formic acid in 5% (v/v) acetonitrile, 95% (v/v) water) and centrifuged for 5 min at 12,000 × *g*. An aliquot of the supernatant (5 μl) was transferred into an autosampling vial. Analyte sampling, chromatography, and production and acquisition of MS/MS data were performed on line using fully automated instrumentation as described in a previous study (36). Double distilled water and HPLC-grade solvents were used throughout the procedure. Analyses of MS/MS data were performed with the Finnigan Sequest/Turbo Sequest software (Rev. 2.0 ThermoQuest, San Jose, CA) using the parameters described in a previous study (36). For MS/MS data evaluation, the *Synechocystis* data base from Kazusa (available at ftp.kazusa.or.jp/pub/cyanobase/Synechocystis) was downloaded (on October 27, 2003) and used.

Blue Native (BN)-PAGE—BN-PAGE through 5–15% (w/v) gradient gels was performed according to a previous study (37). For analysis of the His-tagged NdhJ preparation, 2 μl of a Coomassie Brilliant Blue (CBB) G-250 stock solution (5% (w/v) in 500 mM aminocaproic acid) was added to 30 μl of sample, containing ~25 μg of total protein, in Binding Buffer. For analysis of thylakoid membranes in Fig. 2*c*, 30 μl of thylakoid membranes, at 0.5 mg/ml chlorophyll in UnoQ buffer, were solubilized by addition of a 10% (w/v) β-DM in UnoQ buffer to give a final concentration of 1% (w/v). The sample was left on ice for 10 min, then unsolubilized membranes were removed by centrifugation in a microcentrifuge for 10 min at 4 °C. Just prior to BN-PAGE, CBB G-250 was added from a 5% (w/v) stock in 500 mM aminocaproic acid to give a detergent/Coomassie ratio of 4:1 (w/w). For analysis of solubilized thylakoid extracts the cathode buffer contained 0.02% (w/v) CBB G-250, whereas for the NDH-1 preparation, a concentration of 0.002% (w/v) was used. Protein markers used to calibrate the gel were: thyroglobulin (669 kDa), ferritin (440 kDa), catalase (232 kDa), and bovine serum albumin (69 kDa). For denaturing electrophoresis in the second dimension, a lane from a blue-native gel was incubated at room temperature in 1% (w/v) SDS and 1% (v/v) β-mercaptoethanol for 1 h, briefly washed twice with water to remove excess β-mercaptoethanol, then placed on top of a 12% (w/v) gel for SDS-PAGE using a Tricine buffer system (31). In the case of Fig. 2*d*, thylakoids were prepared and analyzed by BN-PAGE as described in a previous study (38).

Fragmentation of NDH-1 complexes was accomplished using similar conditions to a previous study (39). Briefly 30 μl of the His-tagged NdhJ sample in Binding Buffer was adjusted to pH 7.5 using HCl and made 0.3 M in NaCl. Triton X-100 was then added from a 10% (v/v) stock solution in Binding Buffer to give a final concentration of 0.15% (v/v). The sample was left on ice for 10 min, then analyzed by BN-PAGE as described above.

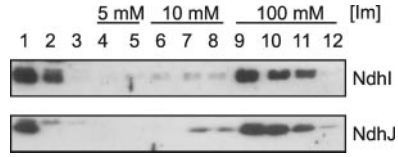

FIG. 1. **Immunoblot analysis of Ni-NTA fractions obtained from the His-tagged NdhJ preparation.** *Lane 1*, pooled fraction from anion-exchange column; *lane 2*, unbound fraction; *lane 3*, wash fraction without imidazole (*Im*); *lanes 4–5*, wash fractions with 5 mM imidazole; *lanes 6–8*, wash fractions with 10 mM imidazole; *lanes 9–12*, fractions obtained by eluting with 100 mM imidazole. Fractions were probed with antibodies specific for NdhI and NdhJ.

NADH and NADPH Dehydrogenase Assays—NADH and NADPH: ferricyanide (FeCN) oxidoreductase activities were assayed at room temperature according to a previous study (40). The decrease in absorbance at 420 nm was assumed to be due to reduction of FeCN. A Shimadzu UV-1601 spectrophotometer was used for all measurements. The assay buffer consisted of 50 mM Tris-HCl, pH 7.5, 0.03% (w/v) β-DM, 0.1 mM NADH or NADPH, and 0.5 mM FeCN.

Bioinformatic Tools—Searches for similar sequences were performed using BLAST programs (41, 42). ChloroP was used to predict whether plant proteins were targeted to the chloroplast (43). The following databases were consulted: The Institute for Genomic Research at www.tigr.org/tdb/, The Arabidopsis Information Resource at www.arabidopsis.org/index.jsp, and CyanoBase at www.kazusa.or.jp/cyano/Synechocystis/index.html.

RESULTS

Isolation of His-tagged NdhJ Preparation—Strain NdhJ-His was constructed by overlap extension PCR so that a His_6 tag was fused to the C terminus of the NdhJ subunit, which is predicted to be a subunit in the interconnecting fragment linking the electron input module to the membrane module ("Experimental Procedures"). Preliminary experiments indicated that Ni-NTA chromatography of a β-DM-solubilized thylakoid membrane extract led to considerable contamination of the NdhJ preparation (data not shown). To help reduce this contamination, the solubilized thylakoid extract was first subjected to anion-exchange chromatography, and pooled fractions containing NdhJ were then purified by Ni-NTA chromatography using imidazole to elute bound NdhJ-containing complexes ("Experimental Procedures"). As the immunoblotting experiment in Fig. 1 shows, both His-tagged NdhJ and the NdhI subunit, which is also predicted to be a component of the interconnecting fragment, were retained by the Ni-NTA resin and were co-eluted with 100 mM imidazole. Control experiments using WT confirmed that non-His-tagged NDH-1 complexes were washed from the resin with 10 mM imidazole (data not shown).

An NDH-1 sub-complex has been identified in previous work as an NAD(P)H dehydrogenase (12). Neither the fractions containing NdhI and NdhJ from the anion-exchange column nor the final His-tagged NdhJ preparation (assayed at 15 μg/ml protein) showed detectable NAD(P)H:ferricyanide oxidoreductase activity (data not shown).

Analysis of the His-tagged NdhJ Preparation by BN-PAGE—The complexity of the His-tagged NdhJ preparation was examined by BN-PAGE. This technique has been applied successfully to the detailed analysis of a variety of membrane-protein complexes, including complex I (44), and possesses the advantages of excellent resolution and of only requiring low amounts of sample (37). One-dimensional BN-PAGE revealed the presence of four Coomassie Blue-staining protein complexes (labeled *A–D* in Fig. 2*a*). The estimated sizes from comparison to a calibration curve were ~460 kDa for complex A, 330 kDa for complex B, 150 kDa for complex C, and 100 kDa for complex D.

To assess the subunit composition of the various complexes, a gel strip obtained by one-dimensional BN-PAGE was sub-

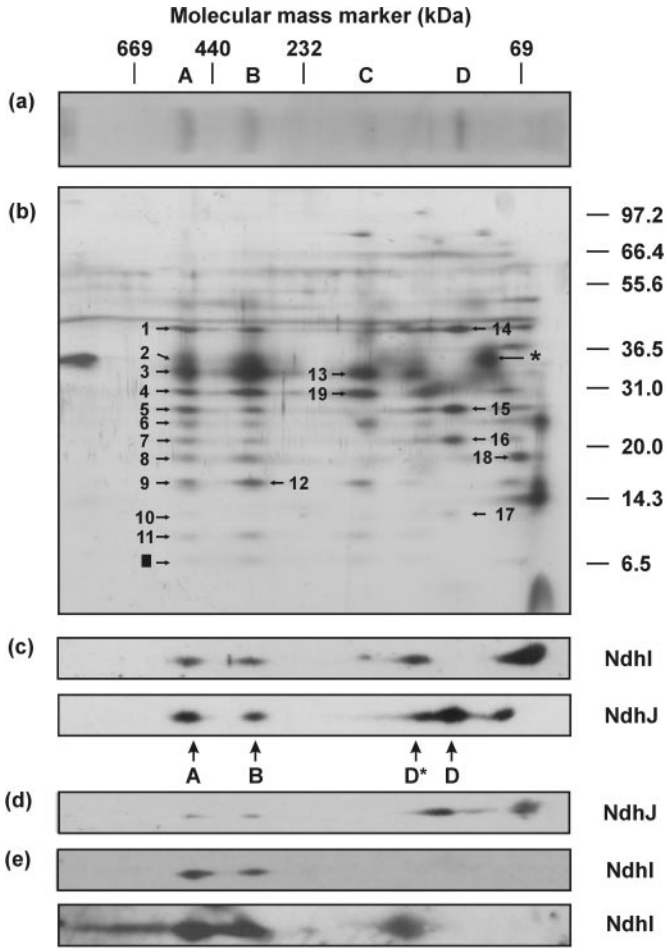

FIG. 2. **Two-dimensional BN-PAGE of the His-tagged NdhJ preparation**. *a*, BN-PAGE in the first dimension was used to resolve complexes *A–D*. *b*, SDS-PAGE was performed in the second dimension, and the gel was visualized by silver stain. Bands referred to in Table I are indicated. The *closed square* indicates position of unassigned low molecular-mass band. The *asterisk* indicates band assigned to NdhD1. *c*, immunoblots using antibodies specific for NdhI and NdhJ. Complex D* is attributed to complex D plus NdhI. *d*, NdhJ immunoblot of solubilized thylakoid membranes from His-tagged NdhJ strain after 2-D BN-PAGE. *e*, NdhI immunoblot of solubilized WT membranes after 2-D BN-PAGE. Lower blot is overexposed blot to indicate presence of smaller NdhI complexes.

jected to SDS-PAGE in the second dimension as described under "Experimental Procedures" (two-dimensional BN-PAGE). Gels were either stained with silver (Fig. 2*b*) or electroblotted to membranes for immunoblotting or N-terminal sequencing.

Inspection of the silver-stained gel in Fig. 2*b* indicated that complexes A and B both showed a similar protein profile, whereas complexes C and D appeared to be sub-complexes derived from complexes A and B. In addition, other very minor complexes could be seen in the silver-stained gel that appeared to contain proteins bands that were found in complexes A and B. However, their low abundance did not allow an accurate assessment of their composition at this stage.

Immunochemical analysis of proteins transferred to nitrocellulose membrane using antibodies specific for NdhI and NdhJ confirmed that both these subunits were both present in complexes A and B (Fig. 2*c*). The NdhJ subunit was also present in complex D and in a second less abundant complex of slightly higher mass than complex D, designated here as D*. The NdhI subunit was also present in D* but appeared to be absent from complex D. Some immunodetectable NdhI and NdhJ subunits migrated with a size of less than 100 kDa in the first dimension. In the case of NdhI, this might reflect the free subunit, whereas NdhJ appeared to remain in a complex.

Assignment of Subunits by N-terminal Sequencing and MS/MS Spectrometry—Unambiguous assignment of the subunits present within complex A, which appeared to the largest NDH-1 complex, and within complex D, was performed by N-terminal sequencing of electroblotted protein. The bands that were analyzed are indicated in the silver-stained gel shown in Fig. 2*b*. The sequencing data obtained for each band is shown in Table I. MS/MS sequencing was also used to identify subunits in bands that failed to yield reliable N-terminal data (Table II). In total, 12 subunits could be identified in the largest NDH-1 complex (complex A).

BN-PAGE of Solubilized Thylakoids from the WT and His-tagged NdhJ Strain—BN-PAGE was performed on solubilized thylakoid membranes from WT and the His-tagged NdhJ mutant to assess the size of the NDH-1 complexes in freshly β-DM-solubilized extracts. As Fig. 2D shows, immunoblots using antibodies specific for NdhJ indicated the presence of two complexes in the His-tagged NdhJ of similar size to complexes A and B observed for the purified His-tagged NdhJ preparation. These data supported the idea that complexes A and B were not artifacts generated by the anion-exchange and Ni-NTA chromatography steps. In addition two smaller complexes similar in size to complex D and D* were detected, but in this case the complex attributed to D* was more abundant than D. For WT membranes the amounts of the smaller complexes were vastly reduced and could only be detected in overexposed immunoblots (Fig. 2*e*). Thus it is possible that the presence of the His tag on NdhJ might be interfering with the assembly of more intact NDH-1 complexes or makes the complex less stable to detergent solubilization or to biochemical manipulation, including freeze/thaw.

Fragmentation of the Large NDH-1 Complexes into Sub-complexes—To examine further the structure of the NDH-1 complexes, the His-tagged NdhJ preparation was treated with Triton X-100 under conditions that fragment *E. coli* complex I (39), and the products analyzed by two-dimensional BN-PAGE (Fig. 3). Fig. 3 confirms that the large NDH-1 complexes were fragmented by the detergent treatment into a number of distinct smaller complexes at the expense of the larger A complex, which had almost disappeared, and the B complex, some of which appeared to be still present in Fig. 3*b* (labeled *B′*). However, whether complex *B′* is identical to complex B or is a different sub-complex of complex A requires further analysis. Table III indicates the assignments of subunits in each complex based on the comparison of mobilities to the gel shown in Fig. 2*b*. Complexes containing the hydrophobic subunits (complexes C and E) and hydrophilic subunits (complexes D and D*) were induced by the detergent treatment. Complex E, which appeared to be derived from complex C by removal of the NdhA subunit, was only clearly detected upon detergent treatment. A large diffuse band migrating at about 36 kDa was also now prominent (indicated by *asterisk* in Fig. 3*b*). Together these data suggested that the NDH-1 complex of *Synechocystis* 6803, like other members of the complex I family, was composed of hydrophobic and hydrophilic modules.

The NdhF3 Subunit Is Not Present in the His-tagged NdhJ Preparation—An interesting feature of *Synechocystis* 6803 and other cyanobacteria is the presence of multiple copies of NdhD and NdhF subunits. For *Synechocystis* 6803 the NdhD3 and NdhF3 subunits have been implicated in the active transport of inorganic carbon into the cell (21). Anti-peptide antibodies specific for NdhF3 were used to assess whether this subunit was actually part of the NDH-J complexes isolated here. As the results in Fig. 4 show, the NdhF3 subunit was detected in

TABLE I

N-terminal sequences and subsequent assignments of subunits found in various NDH-1 complexes

The bands analyzed are numbered in Fig. 2*b*, and the subunit assignment is based on comparison of the determined sequence (a) to the decoded genome sequence (b).

Gel band	Protein sequence	Subunit assignment (CyanoBase designation)	Molecular mass[a]	Apparent molecular mass by SDS-PAGE[b]	*E.coli* homologue (location)[c]
			kDa		
	(a) determined N-terminal sequence (b) deduced from DNA sequence				
1 and 14	(a) TKIETRTE (b) MTKIETRTE[d]	NdhH (slr0261)	45.4	43	NuoCD (peri)
4	(a) MTSGIDLQ (b) MTSGIDLQ	NdhA (sll0519)	40.5	29	NuoH (mem)
5 and 15	(a) PNPANPTD (b) MSPNPANPTD	NdhK (slr1280)	27.1	25	NuoB (peri)
6	(a) MFNNILKQ (b) MFNNILKQ	NdhI (sll0520)	22.2	23	NuoI (peri)
7 and 16	(a) AEEVNSPN (b) MAEEVNSPN	NdhJ (slr1281)	21.3	20	NuoCD (peri)
8 and 18	(a) AMNVKELD (b) AMNVKELD	NdhF1 (slr0844) (Beginning at residue 483)	22.2	18	NuoL (mem)
9	(a) MLPLPLIA (b) MLPLPLIA	sll1262	17.6	15	none
10 and 17	(a) MLVKSTTR (b) MLVKSTTR	slr1623	14.1	12	none
11	(a) MFVLTG (b) MFVLTG	NdhC (slr1279)	13.7	11	NuoA (mem)
12	Mixture of sequences[e]				
	(a) MLP*XXX*IA (b) MLPLPLIA	sll1262	17.6	15	None
	(a) MNLAE*XX*Q (b) MNLAEGVQ	NdhG (sll0521)	21.5	15	NuoJ (mem)

[a] Predicted molecular mass takes into account removal of residues at the N-terminus and addition of His-tag to NdhJ.
[b] Apparent molecular mass was determined by one-dimensional SDS-PAGE not from the gel shown in Fig. 2. The marked deviation between the apparent and predicted molecular masses for NdhA is probably due to its high degree of hydrophobicity.
[c] Location of *E. coli* subunits in either the peripheral arm (peri) or membrane fragment (mem) according to Ref. 4.
[d] The translated sequence for NdhH available in CyanoBase starts at the second Met rather than the first available Met. This means that NdhH is actually 10 residues longer.
[e] Unidentified residues are indicated by *X*.

TABLE II

Identification of Ndh subunits by mass spectrometry

Database used: Synecho_p created 9.7.2003 downloaded 27.10.2003 from Kazusa (ftp.kazusa.or.jp/pub/cyanobase/Synechocystis).

Gel band	Subunit assignment (CyanoBase designation)	Mass[a]	Apparent mass[b]	Z[c]	ΔM[d]	MH^{+}[e]	Xc[f]	ΔCn[g]	Sequence
			kDa						
2	NdhD1 (slr0331)	57.5	36	2	−0.9	2088	4.59	0.67	LITQIYDPTINQLVQTAR
3	NdhB (sll0223)	55.4	33	2	0	1654.8	2.94	0.51	TGSDQISDYAGLYHK
	NdhB (sll0223)			1	0.2	705.2	1.91	0.39	NYPAIK
	NdhB (sll0223)			2	0.8	1653.9	3.40	0.61	TGSDQISDYAGLYHK
	NdhB (sll0223)			1	−0.3	705.7	1.93	0.31	NYPAIK
4	NdhA (sll0519)	40.5	29	2	−0.5	1994.6	4.40	0.60	IGPEYAGPLGVLQPVADGIK
	NdhA (sll0519)			2	−0.8	1245.5	2.94	0.46	LVFKEDVVPAK
	NdhA (sll0519)			2	−0.4	1781.5	2.23	0.45	FLLPVALANLLITAALK
	NdhA (sll0519)			1	−0.1	757.5	2.20	0.41	EDVVPAK
9	sll1262	17.6	15	2	0.1	2164.9	4.30	0.72	ALENDGALAVYAPLEGGYEGR
	NdhG (sll0521)	21.5	15	2	−0.8	1443.5	3.67	0.54	RDLIPELSEENK
19	NdhA (sll0519)	40.5	29	2	−0.2	1994.3	4.66	0.67	IGPEYAGPLGVLQPVADGIK
	NdhA (sll0519)			2	−0.3	1200	3.87	0.45	IDQLLNLGWK
	NdhA (sll0519)			2	−0.7	1245.5	3.39	0.61	LVFKEDVVPAK
	NdhA (sll0519)			1	−0.1	757.6	2.26	0.41	EDVVPAK

[a] Predicted molecular mass.
[b] Apparent molecular mass was determined by one-dimensional SDS-PAGE not from the gel shown in Fig. 2. The marked deviation between the apparent and predicted molecular masses for NdhA, NdhB, and NdhD1 is probably due to their high degree of hydrophobicity.
[c] Charge.
[d] Mass difference between measurement and calculation.
[e] Mass of peptide ion.
[f] Cross-correlation between measured and *in silico* produced fragments.
[g] Difference between best two hits (normalized to 1).

thylakoid membranes but was absent in the final His-tagged NdhJ preparation. Together these data suggest that, if NdhF3 is a subunit of a larger NDH-1 complex containing NdhJ *in vivo*, then such complexes are unstable.

DISCUSSION

The His Tag on NdhJ Does Not Drastically Impair NDH-1 Function—This report describes the construction of a strain of *Synechocystis* 6803 in which the C terminus of the NdhJ sub-

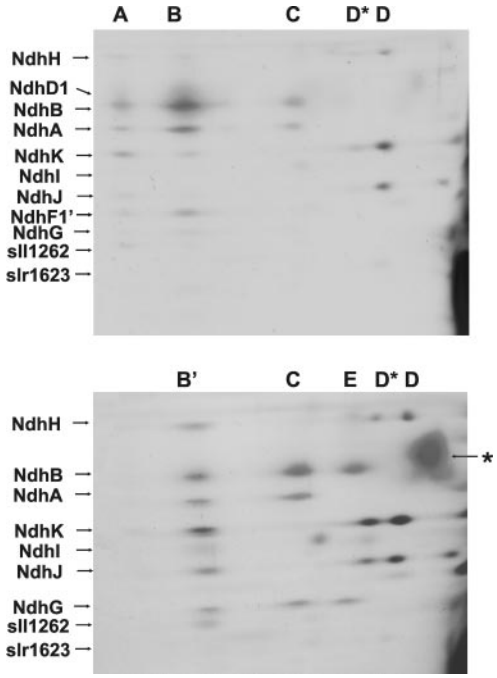

FIG. 3. **Fragmentation of NDH-1 complexes.** The NDH-1 complexes were examined by two-dimensional BN-PAGE before (*a*) and after (*b*) treatment with Triton X-100 as described under "Experimental Procedures." Subunits were assigned by comparison to the gel shown in Fig. 2*b*. The *asterisk* indicates band assigned to NdhD1. Position of NDH-1 complexes (*A–E*) indicated. Complexes *B* and *B′* show similar electrophoretic mobilities but might have different subunit compositions.

TABLE III
Proposed subunit composition of the NDH-1 complexes separated by BN-PAGE

Letters indicate the *ndh* gene product.

Complex	Subunit composition
A	2x (H, I, J, K, slr1623, sll1262) plus A, B, C, D, E, F′, G
B	(H, I, J, K, slr1623, sll1262) plus A, B, C, D, E, F′, G
C	A, B, C, E, G
D	H, J, K, slr1623
D*	H, I, J, K, slr1623
E	B, G, C, E

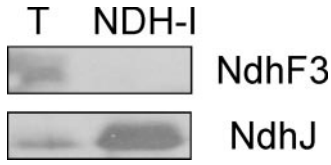

FIG. 4. **NdhF3 is not present in the His-tagged NdhJ preparation.** Solubilized thylakoid membranes (*T*) and the final purified His-tagged NdhJ preparation (*NDH-1*) were immunoblotted with antibodies specific for NdhF3 and NdhJ.

unit has been engineered to contain a His tag. The mutant grows as well as the WT in liquid cultures and on agar plates at ambient CO_2 levels (data not shown). Given that many *ndh* insertion mutants are usually only able to grow in the presence of elevated levels of CO_2 (13, 21), it is unlikely that the incorporation of the affinity tag has drastically affected the activity of the NDH-1 complex in this strain. Immunoblots also indicated that the levels of NdhJ were similar in membranes from WT and the His-tagged mutant (data not shown).

Detection of Large NDH-1 Complexes and Identification of Two New Ndh Subunits—BN-PAGE in combination with SDS-PAGE and protein sequencing has proved highly effective in assessing the size and subunit composition of the protein complexes present in the His-tagged NdhJ preparation. The largest NDH-1 complex, termed here complex A, has an apparent mass of about 460 kDa. Approximately 11 protein bands could be resolved in complexes A and B, and 12 subunits could be identified. Importantly complex A appears to contain Ndh subunits that have been predicted to be peripheral to the membrane (NdhH, -I, -J, and -K) as well as subunits that are predicted to be intrinsic to the membrane (NdhA, -B, -C, -D1, -F1, and -G). Our data therefore provide the first clear evidence for the participation of these Ndh subunits in a single complex. Overall the size of complex A is close to that of the minimal type of complex I found in *E. coli* (6).

Importantly our data identify the presence of two new Ndh subunits, designated in CyanoBase as slr1623 and sll1262. As outlined in the introduction, Steinmüller and colleagues (25) first detected slr1623 (or the 14-kDa subunit) following immunoprecipitation experiments using antibodies specific for NdhK. Unfortunately, they could not exclude the possibility that it was a contaminant or involved in the assembly of NDH-1 complexes. The identification of slr1623 in the largest NDH-1 complex described here now confirms its assignment as an *ndh* gene product. The complete sequence alignments shown in Fig. 5 lend some support to the suggestion by Berger *et al.* (25), based on the determined sequence of the first 10 amino acids, that slr1623 is related to subunit B13 of the bovine complex I. B13 is found in the same hydrophilic sub-complex of complex I, designated Iλ, as the bovine homologues of NdhH, -K, and -J (49-kDa subunit, PSST, and 30-kDa subunits, respectively), but its role is unknown (45). The sll1262 subunit has never been implicated before as an Ndh subunit and does not have obvious relatives in the mitochondrial or minimal forms of complex I. For both slr1623 and sll1262 there are no obvious sequence motifs that would suggest a possible function.

Repeated attempts to sequence the band migrating at ~7 kDa in Fig. 2*b* (indicated by a *closed square*) have been unsuccessful. Based on size, NdhE and possibly NdhL are promising candidates (17). A C-terminal fragment of NdhF1 was found in complex A, but it remains unclear whether it is a component of the NDH-1 complex *in vivo* or is an isolation artifact.

Although NAD(P)H:ferricyanide oxidoreductase activity was detected in the solubilized thylakoid extract, no detectable NADH or NADPH:ferricyanide oxidoreductase activities were found to co-purify with the NdhI and NdhJ subunits following anion-exchange chromatography. If the NDH-1 complex is truly an NAD(P)H dehydrogenase, then this activity would appear to be highly labile or easily detached from the rest of the complex.

NDH-1 Is Composed of Hydrophilic and Hydrophobic Modules—Comparison of the protein profiles in the two-dimensional gels (Figs. 2*b* and 3) reveals that the larger NDH-1 complexes (complexes A and B) can be fragmented into smaller yet stable sub-complexes (complexes C, D, D*, and E). This is most apparent after detergent-induced fragmentation (Fig. 3), but their presence can still be detected at lower level in the control samples (Figs. 2*b* and 3*a*). Thus some fragmentation of the NDH-1 complex appears to have occurred during isolation and/or during BN-PAGE, consistent with the known instability of NDH-1 (12, 25). In the case of complex D, it is also possible that it represents a stable assembly intermediate.

Complex D contains NdhH, -J, -K, and slr1623. The immunochemical data in Fig. 2*c* indicated that complex D does not in fact contain the NdhI subunit. NdhI is more easily removed upon fragmentation of NDH-1 so that the abundance of the sub-complex consisting of complex D plus attached NdhI (D*, *arrowed* in Fig. 2*c*) is rather low. For solubilized thylakoid membranes, the amount of complex D* appears to be greater

```
                    *         20         *         40
slr1623 : --MLVKSTTRHVRIFSAEVQGNELIPSNNVLTMDVDPDNEFVWNE :  43
B13     : MAGLLKKTTGLV-GLAVCDTPHERLT--ILYTKTLDILKHFP-KH :  41

               *         60         *         80         *
slr1623 : DALQQVYRRFD-ELVESYSGE-DLTDYNLRRIGSDLEHFIRDLLQ :  86
B13     : AAYRKYTEQITNEKLDMVKAEPDVKKLEALLQGGEVEEVI--L-Q :  83

                   100         *         120
slr1623 : AGKVSYNLDCRVLNYSMGLPKVENQETAGKYWLDN : 121
B13     : AEK-ELSLARKMLKWKPWEPLVEEPPANQWKWPI- : 116
```

FIG. 5. **Sequence comparison between slr1623 (*Synechocystis* sp. PCC 6803) and complex I subunit B13 (*Bos taurus*) (P23935).** The *boxes* show similar residues in these two sequences.

than that of complex D, so it is likely that NdhI becomes detached during biochemical purification (Fig. 2*d*).

Complex C appears to contain most of the subunits found in complexes A and B after the removal of the hydrophilic sub-complex (NdhH, -I, -J, -K, and slr1623), sll1262 and the C-terminal fragment of NdhF1, which was detected in the low molecular mass region of the blue native gel (*band 18* in Fig. 2*b*). By analogy to *E. coli* and bovine complex Is, complex C represents a hydrophobic sub-complex buried in the membrane. Comparison of the protein profile for complex C to that of complex A indicates that band 2 (indicated in Fig. 2*b* and shown to contain NdhD1) is also missing. A diffuse band of similar mobility can be identified migrating in the low molecular mass range of the gel (shown as an *asterisk* in Fig. 2*b*), particularly in the fragmentation experiment presented in Fig. 3*b*. That NdhD1 and the C-terminal fragment of NdhF1 can be removed relatively easily from NDH-1 complexes is consistent with the fact that their homologues in complex I from bovine mitochondria (ND4 and ND5) and *E. coli* (NuoM and NuoL) lie at the distal end of both hydrophobic sub-complexes and are also more easily detached (39, 45). Complex E, detected in Fig. 3*b* but also observed at lower level in Fig. 2*b*, has a similar gel profile to complex C except that the NdhA subunit is absent. This is reflected in the observed difference in mass between complexes C and E of about 30 kDa.

A model to explain the interrelationships of the various sub-complexes and their subunit composition is presented in Fig. 6 and Table III. Overall, our results are in agreement with current models for the structure of prokaryotic complex I, such as that from *E. coli* (39), except that the electron input module is not conserved. Given the possible errors involved in measuring the masses of the complexes by BN-PAGE, we cannot yet discount the possibility that some of the complexes that we observe are actually dimers or contain multiple copies of some of the subunits.

The newly discovered Ndh subunit, sll1262, was detected in both complexes A and B, where it migrates close to the NdhG subunit. Based on the variation of staining intensity between complex A and B (discussed below), sll1262 is assigned to the hydrophilic sub-complex. However, like NdhI, it is absent from complex D, so sll1262 would appear to be more easily removed from the hydrophilic sub-complex.

Stoichiometry of the Modules—Complexes A (460 kDa) and B (330 kDa) show similar protein profiles by SDS-PAGE yet show considerable differences in size. One possibility is that complex A represents a dimer of complex B. However, the apparent size for A of 460 kDa is much smaller than that for the predicted dimer (660 kDa). Visual inspection of the silver-stained gels, particularly in Fig. 3*a*, reveals that there is a significant difference in the relative staining intensity of the protein bands found in complex A and complex B. The staining intensity of the hydrophilic subunits (NdhH, -I, -J, and -K), relative to that of the hydrophobic subunits (*e.g.* NdhD1, -B, -A, and -F1′), is much greater in complex A than in complex B. If A were a dimer of B, then there should be no difference in relative staining intensity. Consequently, it seems likely, given their

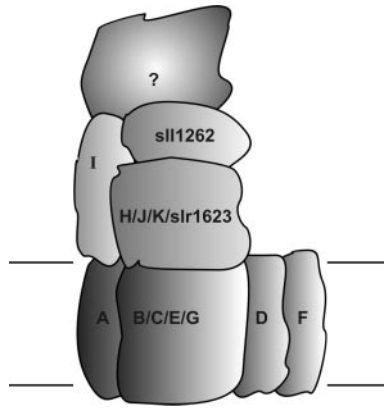

FIG. 6. **A model of the Ndh subunit arrangement in complex B.** *Letters* indicate the Ndh subunit. Unknown electron input module indicated by the *question mark*.

apparent sizes, that complex A represents an NDH-1 complex in which there are two hydrophilic sub-complexes per hydrophobic sub-complex and that complex B is a complex in which 1 of the hydrophilic sub-complexes has been removed. The molecular mass of the hydrophilic sub-complex consisting of NdhH, -K, -I, -J, slr1623, and sll1262 is about 150 kDa. This agrees fairly well with the difference in size between complexes A (460 kDa) and B (330 kDa). Given that similar sized complexes to A and B were found in solubilized thylakoids (Fig. 2, *d* and *e*), the variable stoichiometry of hydrophilic and hydrophobic sub-complexes might be physiologically relevant.

At the moment complex I from mitochondria and *E. coli* is considered to be composed of one copy of the peripheral arm (composed of the NADH-oxidizing sub-complex and the interconnecting fragment) to one copy of the hydrophobic domain, arranged in a 'L'-shaped configuration (reviewed previously (5, 46)). However, little work has been directed at determining the stoichiometry of the hydrophobic and hydrophilic subunits within native complex I. Consequently, it remains unclear the degree to which highly purified complex I preparations have fragmented during isolation. The possibility that monomeric complex I might contain two copies of the key hydrophilic modules cannot be discounted and might help explain why recent measurements indicate that there are two FMN and two N2 Fe-S clusters per monomeric complex I (47). However, given that the apparent molecular masses determined by BN-PAGE might vary significantly from the true masses, it also remains possible that complex A is an NDH-1 dimer and that complex B has lost one of the hydrophilic modules.

Our immunochemical identification of two large NDH-1 complexes in thylakoid membranes agrees with a recent proteomics analysis by Herranen and colleagues (24). They also detected two large NDH-1 complexes (designated NDH-1L and NDH-1M) of similar size to complexes A and B described here. Both NDH-1L and NDH-1 M were shown to contain the NdhH, -I, -J, and -K subunits; however, the remaining subunits were not identified.

TABLE IV
Identification of higher plant orthologues of slr1623 and sll1262

Synechocystis 6803 subunit (predicted number of amino acid residues)	*Arabidopsis* entry (predicted number of amino acid residues in precursor/mature form)	BLAST	*Zea mays* entry (predicted number of amino acid residues in precursor/mature form)	BLAST	Protein sequence of *Z. mays* ((a) N-terminal sequence from chloroplast Ndh prep (50) (b) deduced from cDNA sequence)
		E value		*E value*	
slr1623 (121)	At4g37920 (673/652)	4E-20	TC195947 GB#CD990821	6.8E-20	(a) AQQEQQVKEEEEAEVA (23.5-kDa subunit) (b) AQQEQQVKEEEAEVA
sll1262 (161)	At5g58260 (209/164)	8E-29	TC195620 GB#AY108360 (208/168)	2.3E-25	(a) STVWDFVGGDLVRPDLK (19-kDa subunit) (b) STVWDFVGGDLVRPDLG

Role of the Different Members of the NdhD and NdhF Families in NDH-1 Function—The data in Fig. 4 indicate that NdhF3 is not present in the NDH-1 complexes isolated here. This would suggest that either NdhF3 is weakly attached to complexes containing NdhJ and is readily removed or that NdhF3 is not actually part of the NDH-1 complex. Strong evidence to support the latter possibility has come from the recent detection of an approximate 180-kDa complex in solubilized thylakoid membranes, termed NDH-1S_1, containing NdhD3 and NdhF3 plus CupA and sll1735, but lacking other NDH-1 subunits (24). This complex appears to be involved in CO_2 uptake but not electron transfer (16). It therefore seems likely that some of the annotated NdhD and NdhF subunits actually have roles unrelated to NDH-1 function. This is not surprising, because the NdhD and NdhF subunits, as well as NdhB, are related to the MrpA-type of antiporter involved in pH homeostasis in *Bacillus subtilis* (48). Indeed phylogenetic analyses indicate that two annotated *ndh* genes, *ndhD5* and *ndhD6*, probably encode antiporters and are not true NDH-1 subunits (49). Overall only NdhD1, NdhD2, and NdhF1 might play a role in NDH-1 function (16).

Identification of the First Nuclear-encoded Subunits of the Chloroplast Ndh Complex—BLAST searches against the complete genome sequence of *Arabidopsis thaliana* identified closely related sequences to both sll1262 and slr1623 (Table IV). According to ChloroP, both the *Arabidopsis* gene products are targeted to the chloroplast and are hence excellent candidates for nuclear-encoded subunits of the chloroplast Ndh complex.

Confirmation that the higher plant homologues of sll1262 and slr1623 are actually chloroplast Ndh subunits comes from a BLAST analysis of the maize genome sequence coupled to N-terminal sequence data obtained from proteins found in a maize chloroplast Ndh preparation (50). Again sequences related to sll1262 and slr1623 can be identified in the maize genome (Table IV). For both these sequences, excellent matches can be obtained with N-terminal sequence data obtained for two abundant proteins found in the Ndh preparation (50) (Table IV). Because there were still some contaminants in the maize preparation, Funk and co-workers were unable to assign these particular subunits unambiguously to the Ndh complex. However, in light of the data presented here, we can now conclude that these are indeed two new nuclear-encoded subunits of the chloroplast Ndh complex. We suggest that slr1623 and sll1262 (and their homologues in plants) be designated NdhM and NdhN, respectively.

Of interest is the finding that there is some variation in size in the higher plant homologues. For *Arabidopsis* the most closely related sequence to slr1623 (At4g37920) contains a 334-amino acid extension at the C terminus, whereas for maize and rice (data not shown) this extension is absent. Instead the extension might exist as a separate subunit within the Ndh complex of these plants. No obvious homologue to this extension exists in cyanobacteria. This would indicate that there are structural and possible functional differences between the cyanobacterial NDH-1 and chloroplast Ndh complexes.

Evolution of the NDH-1 Complex and the Nature of the Electron Input Module—The NDH-1 complexes isolated here fail to show detectable NAD(P)H:FeCN oxidoreductase activity. This would suggest that the activity is extremely labile or that the NDH-1 complex is not actually an NAD(P)H dehydrogenase as often assumed in the literature. Evidence to support a role in NADPH oxidation has come mainly from the comparison of activities in thylakoid membranes isolated from WT to those from the M55 mutant (lacking an intact NdhB subunit) (14) and the partial purification of a hydrophilic sub-complex of NDH-1 (12). A defined NDH-1 complex possessing NAD(P)H dehydrogenase activity has not yet been characterized.

Currently, the nature of the electron input module of NDH-1 is unknown. A number of candidates have been suggested for cyanobacterial NDH-1, including hydrogenase subunits HoxF and HoxU, which are related to the NADH-oxidizing sub-complex of complex I (8, 9), and ferredoxin (6). It is also possible that there are multiple modules. Given that homologues of slr1623 and sll1262 are not found in the minimal type of complex I, the presence of these subunits in NDH-1 might reflect differences in the nature of the electron-input module. For instance sll1262 might be involved in binding substrate, such as reduced ferredoxin, or a larger module, to the NDH-1 complex. For the chloroplast Ndh complex, suggested input devices include FNR (50, 51) and nuclear-encoded homologues of NuoE, -F, and -G, which might be targeted to both the mitochondrion and the chloroplast (52). Isolation of the chloroplast Ndh complex using the His-tagging strategy described here might be a useful way to investigate its structure in the future.

According to Friedrich and colleagues (3, 4), complex I of eubacteria and mitochondria has evolved from pre-existing modules that were adapted to NADH oxidation, quinone reduction, and the pumping of protons. A close homologue to complex I has recently been characterized in a methanobacterium (53) and a sulfate-reducing bacterium (54). Like the thylakoid NDH-1 complex, the archaebacterial complexes possess homologous subunits to the membrane and interconnecting fragments of the classic NADH-oxidizing complex I. But instead of an NADH-oxidizing module, they contain a single subunit that is involved in the oxidation of coenzyme $F_{420}H_2$, a 5-deazaflavin derivative. We have identified using BLAST searches highly related gene products to this archaebacterial electron input device (designated FpoF in *Methanosarcina mazei*) in both cyanobacteria (slr1923 in *Synechocystis* 6803; *E* value of $8E-17$) and in higher plants (At1g04620.1 in *A. thaliana*; *E* value of $7.8E-11$). In the latter case the gene product is predicted by ChloroP to be targeted to the chloroplast. Hence, by analogy, we suggest that these particular subunits should also be considered as possible electron input modules for the thylakoid NDH-1 and Ndh complexes, respectively. Whether they still oxidize coenzyme $F_{420}H_2$ or have evolved to use alternative substrates, such as NAD(P)H, is an open question that can be tested.

Acknowledgments—We are grateful to Prof. E.-M. Aro for sending antibodies to NdhF3 and to Dr. Josef Komenda (Trebon, Czech Republic) for preparing the membrane filter used in Fig. 2*e*.

REFERENCES

1. Ohkawa, H., Sonoda, M., Shibata, M., and Ogawa, T. (2001) *J. Bacteriol.* **183,** 4938–4939
2. Kaneko, T., Sato, S., Kotani, H., Tanaka, A., Asamizu, E., Nakamura, Y., Miyajima, N., Hirosawa, M., Sugiura, M., Sasamoto, S., Kimura, T., Hosouchi, T., Matsuno, A., Muraki, A., Nakazaki, N., Naruo, K., Okumura, S., Shimpo, S., Takeuchi, C., Wada, T., Watanabe, A., Yamada, M., Yasuda, M., and Tabata, S. (1996) *DNA Res.* **3,** 109–136
3. Friedrich, T., and Weiss, H. (1997) *J. Theor. Biol.* **187,** 529–540
4. Friedrich, T., and Scheide, D. (2000) *FEBS Lett.* **479,** 1–5
5. Brandt, U., Kerscher, S., Dröse, S., Zwicker, K., and Zickermann, V. (2003) *FEBS Lett.* **545,** 9–17
6. Friedrich, T., Steinmüller, K., and Weiss, H. (1995) *FEBS Lett.* **367,** 107–111
7. Nixon, P. J. (2000) *Philos. Trans. R Soc. Lond. B Biol. Sci.* **355,** 1541–1547
8. Appel, J., and Schulz, R. (1996) *Biochim. Biophys. Acta* **1298,** 141–147
9. Schmitz, O., and Bothe, H. (1996) *Naturwissenschaften* **83,** 525–527
10. Berger, S., Ellersiek, U., and Steinmüller, K. (1991) *FEBS Lett.* **286,** 129–132
11. Mi, H., Endo, T., Ogawa, T., Asada, K. (1995) *Plant Cell Physiol.* **36,** 661–668
12. Matsuo, M., Endo, T., and Asada, K. (1998) *Plant Cell Physiol.* **39,** 263–267
13. Ogawa, T. (1991) *Proc. Natl. Acad. Sci. U. S. A.* **88,** 4275–4279
14. Mi, H., Endo, T., Schreiber, T., Ogawa, T., and Asada, K. (1992) *Plant Cell Physiol.* **33,** 1233–1238
15. Cooley, J. W., and Vermaas, W. F. (2001) *J. Bacteriol.* **183,** 4251–4258
16. Badger, M., and Price, G. D. (2003) *J. Exp. Bot.* **54,** 609–622
17. Ogawa, T. (1992) *Plant Physiol.* **99,** 1604–1608
18. Pieulle, L., Guedeney, G., Cassier-Chauvat, C., Jeanjean, R., Chauvat, F., and Peltier, G. (2000) *FEBS Lett.* **487,** 272–276
19. Nakamura, Y., Kaneko, T., Hirosawa, M., Miyajima, N., and Tabata, S. (1998) *Nucleic Acids Res.* **26,** 63–67
20. Klughammer, B., Sültemeyer, D., Badger, M. R., and Price, G. D. (1999) *Mol. Microbiol.* **32,** 1305–1315
21. Ohkawa, H., Pakrasi, H. B., and Ogawa, T. (2000) *J. Biol. Chem.* **275,** 31630–31634
22. Ohkawa, H., Price, G. D., Badger, M. R., and Ogawa, T. (2000) *J. Bacteriol.* **182,** 2591–2596
23. Shibata, M., Ohkawa, H., Kaneko, T., Fukuzawa, H., Tabata, S., Kaplan, A., and Ogawa, T. (2001) *Proc. Natl. Acad. Sci. U. S. A.* **98,** 11789–11794
24. Herranen, M., Battchikova, N., Zhang, P., Graf, A., Sirpiö, S., Paakkarinen, V., and Aro, E.-M. (2004) *Plant Physiol.* **134,** 470–481
25. Berger, S., Ellersiek, U., Kinzelt, D., and Steinmüller, K. (1993) *FEBS Lett.* **326,** 246–250
26. Deng, Y., Ye, J., and Mi, H. (2003) *Plant Cell Physiol.* **44,** 534–540
27. Kashani-Poor, N., Kerscher, S., Zickermann, V., and Brandt, U. (2001) *Biochim. Biophys. Acta* **1504,** 363–370
28. Ho, S. N., Hunt, H. D., Horton, R. M., Pullen, J. K., and Pease, L. R. (1989) *Gene* (*Amst.*) **77,** 51–59
29. Williams, J. G. K. (1988) *Methods Enzymol.* **167,** 766–778
30. Wellburn, A. R., and Lichtenthaler, H. (1984) in *Advances in Photosynthesis Research* (Sybesma, C., ed) Vol. II, pp. 9–12, Nijhoff/Junk, The Hague
31. Schägger, H., and von Jagow, G. (1987) *Anal. Biochem.* **166,** 368–379
32. Burrows, P. A., Sazanov, L. A., Svab, Z., Maliga, P., and Nixon, P. J. (1998) *EMBO J.* **17,** 868–876
33. Blum, H., Beier, H., and Gross, H. (1987) *Electrophoresis* **8,** 93–99
34. Dunn, S. (1986) *Anal. Biochem.* **157,** 144–153
35. Mortz, E., Vorm, O., Mann, M., and Roepstorff, P. (1994) *Biol. Mass Spectrom.* **23,** 249–261
36. Stauber, E., Fink, A., Markert, C., Kruse, O., Johanningmeier, U., and Hippler, M. (2003) *Eukaryot. Cell* **2,** 978–994
37. Schägger, H., Cramer, W. A., and von Jagow, G. (1994) *Anal. Biochem.* **217,** 220–230
38. Tichý, M., Lupínková, L., Sicora, C., Vass, I., Kuviková, S., Prášil, O., and Komenda, J. (2003) *Biochim. Biophys. Acta* **1605,** 55–66
39. Holt, P. J., Morgan, D. J., and Sazanov, L. A. (2003) *J. Biol. Chem.* **278,** 43114–43120
40. Galante, Y. M., and Hatefi, Y. (1979) *Arch. Biochem. Biophys.* **192,** 559–568
41. Altschul, S. F., Gish, W., Miller, W., Myers, E. W., and Lipman, D. J. (1990) *J. Mol. Biol.* **215,** 403–410
42. Altschul, S. F., Madden, T. L., Schaffer, A. A., Zhang, J., Zhang, Z., Miller, W., and Lipman, D. J. (1997) *Nucleic Acids Res.* **25,** 3389–3402
43. Emanuelsson, O., Nielsen, H., and von Heijne, G. (1999) *Protein Sci.* **8,** 978–984
44. Heazlewood, J. L., Howell, K. A., and Millar, A. H. (2003) *Biochim. Biophys. Acta* **1604,** 159–169
45. Sazanov, L. A., Peak-Chew, S. Y., Fearnley, I. M., and Walker, J. E. (2000) *Biochemistry* **39,** 7229–7235
46. Hirst, J., Carroll, J., Fearnley, I. M., Shannon, R. J., and Walker, J. E. (2003) *Biochim. Biophys. Acta* **1604,** 135–150
47. Albracht, S. P. J., van der Linden, E., and Faber, B. W. (2003) *Biochim. Biophys. Acta* **1557,** 41–49
48. Ito, M., Guffanti, A., Oudega, B., and Krulwich, T. (1999) *J. Bacteriol.* **181,** 2394–2402
49. Mathiesen, C., and Hägerhäll, C. (2002) *Biochim. Biophys. Acta* **1556,** 121–132
50. Funk, E., Schäfer, E., and Steinmüller, K. (1999) *J. Plant Physiol.* **154,** 16–23
51. Guedeney, G., Corneille, S., Cuiné, S., and Peltier, G. (1996) *FEBS Lett.* **378,** 277–280
52. Quiles, M., Garcia, A., and Cuello, J. (2003) *Plant Sci.* **164,** 541–547
53. Bäumer, S., Ide, T., Jacobi, C., Johann, A., Gottschalk, G., and Deppenmeier, U. (2000) *J. Biol. Chem.* **275,** 17968–17973
54. Brüggemann, H., Falinski, F., and Deppenmeier, U. (2000) *Eur. J. Biochem.* **267,** 5810–5814